

1 **Removing spurious low-frequency variability in drifter velocities**

2 **RICK LUMPKIN ***

NOAA's Atlantic Oceanographic and Meteorological Laboratory, Miami, FL USA 33149

3 **SEMYON A. GRODSKY**

Department of Atmospheric and Oceanic Science, University of Maryland, College Park, MD 20742

4 **LUCA CENTURIONI**

Scripps Institution of Oceanography, San Diego, La Jolla CA 92093

5 **MARIE-HELENE RIO**

CLS, Space Oceanography Division, Toulouse, France

6 **JAMES A. CARTON**

Department of Atmospheric and Oceanic Science, University of Maryland, College Park, MD 20742

7 **DONGKYU LEE**

Department of Oceanography, Pusan National University, Busan, Korea

* *Corresponding author address:* Rick Lumpkin, NOAA/AOML, 4301 Rickenbacker Cswy, Miami, FL 33149.

E-mail: Rick.Lumpkin@noaa.gov

ABSTRACT

9 Satellite-tracked drifting buoys of the Global Drifter Program have drogues, centered at 15 m
10 depth, to minimize direct wind forcing and Stokes drift. Drogue presence has historically
11 been determined from submergence or tether strain records. However, recent studies have
12 revealed that a significant fraction of drifters believed to be drogued have actually lost their
13 drogues, a problem which peaked in the mid-2000s before the majority of drifters in the global
14 array switched from submergence to tether strain sensors. In this study, a methodology is
15 applied to the data to automatically reanalyze drogue presence based on anomalous down-
16 wind ageostrophic motion. Results indicate that the downwind slip of undrogued drifters is
17 approximately 50% higher than previously believed. The reanalyzed results no longer exhibit
18 the dramatic and spurious interannual variations seen in the original data. These results,
19 along with information from submergence/tether strain and transmission frequency varia-
20 tions, are now being used to conduct a systematic manual reevaluation of drogue presence
21 for each drifter in the post-1992 data set.

22 1. Introduction

23 Satellite-tracked drifting buoys (hereafter “drifters”) of the Global Drifter Program (GDP)
24 have been collecting near-surface ocean current observations in the tropical Pacific since 1979,
25 with observations in the other basins also now spanning more than 15 years. The GDP is
26 a branch of NOAA’s Global Ocean Observing System and a scientific project of the Data
27 Buoy Cooperation Panel, and is funded by NOAA’s Climate Program Office. Its objectives
28 are to maintain a global array of ~ 1250 drifters and to provide a data processing system for
29 scientific use of the resulting observations, which support short-term (seasonal to interan-
30 nual) climate predictions, climate research, and climate monitoring. A subset of the drifters
31 also include barometers for improved numerical weather forecasting efforts. The GDP works
32 with a large number of national and international partners in order to fulfill these goals.¹

33 Drifter data allow investigators to explore short-term climate variability of the ocean
34 circulation and understand how it responds to changing surface forcing. However, recent
35 studies have reported evidence of spurious variations in drifter-derived surface currents in the
36 mid-2000s (Grotsky et al., 2011 [hereafter GLC11]; Rio et al., 2011; Piecuch and Rynearson,
37 2012). These spurious variations became detectable in 2003, reached peak severity in 2006–
38 2007, and subsequently diminished (Fig. 1). GLC11 have shown that these variations have a
39 pattern similar to mean surface winds, and may be explained by the presence of undiagnosed
40 drogue loss whose occurrence changes in time.

41 GDP drifters have a drogue (sea anchor) centered at 15 m depth so that their trajectories
42 reflect near-surface ocean currents (Niiler 2001; Lumpkin and Pazos 2007). When the drogue
43 is attached, the downwind “slip” (drifter motion with respect to water motion at 15 m) is
44 $\sim 0.1\%$ of the wind speed for winds up to 10 m/s (Niiler et al. 1995); when it is lost, slip
45 increases to $\sim 1\%$ of the wind speed (Pazan and Niiler 2001; Poulain et al. 2009). This
46 increase is due to a combination of wind drag on the surface float, the vertical shear of
47 wind-driven currents, and wave-induced Stokes drift within the upper 15 m.

¹For more information, see <http://www.aoml.noaa.gov/phod/dac/gdp/objectives.php>.

48 Drogue presence is determined by submergence from a pair of sensors near the top of the
49 drifter’s surface float, or by a tether strain sensor at the base of the float. The more recent
50 and accurate tether strain was developed in the early 2000s, and phased in for the entire
51 drifter array in the period 2008–2010. Current statistics from drogue-off drifters indicate
52 that $\sim 30\%$ of drifters lose their drogues in the first three months of deployment while nearly
53 90% lose their drogues in the first 1.5 years. To minimize the effect of undiagnosed drogue
54 loss, GLC11 recommended using velocities from only the first three months of data currently
55 identified as drogue-on for the period January 2004–December 2008, until a full reanalysis
56 of drogue presence could be performed. However, this interim solution eliminates $\sim 75\%$ of
57 the velocity data currently identified as drogue-on during this period.

58 The main motivation of this study is to provide the oceanographic community with a high
59 quality dataset of ocean currents at 15 m depth. Velocity data from drifters are often used,
60 for example, to validate surface currents in global and regional ocean circulation models and
61 it is therefore crucial to remove biases from the historical archive. In this study we adapt
62 a methodology developed by Rio (2012) to automatically reassess drogue presence for each
63 drifter in the historical data set since the start of continuous satellite altimetry on 14 October
64 1992. We demonstrate the effects of this reanalysis upon time-mean and low-frequency
65 variations in drifter velocities, and demonstrate that it significantly reduces the spurious
66 low-frequency variations. We also demonstrate that drogue presence from submergence can
67 be reevaluated when examined concurrently with the results of the new methodology, and
68 that another signal – transmission frequency variations – can serve as a third drogue presence
69 indicator. We conclude by describing how these indicators are currently being implemented
70 by the GDP to improve the quality of the drifter data.

71 2. Data and methods

72 Surface velocities are calculated from the quality controlled, 6 h interpolated drifter
73 positions (Hansen and Poulain 1996) via 12-h centered differencing. The data set in the
74 time period 14 October 1992–11 November 2010 consists of 13,593 unique drifters.

75 Sea height anomalies are derived from the $1/3^\circ$ gridded Ssalto/Duacs delayed-time up-
76 dated (up to four satellites) altimeter product of Archiving, Validation, and Interpretation
77 of Satellite Oceanography (AVISO) (Le Traon et al. 1998). The start date of these data
78 set the date for the earliest drifters considered here, and considerably predates the onset of
79 drogue detection problems (Fig. 3 of GLC11). Time-mean sea height is obtained from the
80 Centre National d’Etudes Spatiales-CLS09 Mean Dynamic Topography (MDT) product (Rio
81 et al. 2011). Surface winds at 6 h, 0.25° resolution are obtained from the Cross-Calibrated
82 Multi-Platform (CCMP) product (Atlas et al. 2011), derived through cross-calibration and
83 merging of ocean surface wind observations using a variational analysis method. Wind
84 stress was calculated from CCMP wind speeds using the COARE3.0 algorithm (Fairall et al.
85 2003). Geostrophic currents are calculated from total sea height (AVISO plus MDT) using
86 the methodology of Lagerloef et al. (1999).

87 *a. Automatic drogue detection reanalysis*

88 The methodology used here to automatically detect drogue loss is based closely on Rio
89 (2012). First, a model of the wind-driven motion of a drogued drifter is calculated as follows,
90 using only drifters which are currently flagged as drogued and, for those after the year 2000,
91 are less than 90 days old (this is more strict than the criterion recommended by GLC11 to
92 be conservative). Geostrophic velocities are interpolated to drifter locations and subtracted
93 from the in situ velocities; the resulting residual velocity components u' , v' and wind stress
94 τ , also interpolated to the drifter locations, are low-passed with a period cut-off of 5 days
95 to eliminate inertial, diurnal and tidal motions. These residual velocities are then grouped

96 in 2° (zonal) by 5° (meridional) by 1 climatological month bins. In each bin, a least squares
 97 best fit for the downwind velocity component u' is found of the form $u' = a\sqrt{\tau}$ and left-of-
 98 wind velocity component $v' = b\sqrt{\tau}$. In general, this statistical fitting of the ageostrophic
 99 drifter currents follows the Ralph and Niiler (1999) and Centurioni et al. (2009) approach
 100 of the form $u' \sim \sqrt{\tau/|f|}$. The latitudinal variations of the fitting coefficients a, b account
 101 for the Coriolis effect (while remaining finite on the equator), while the spatial and monthly
 102 variations allow for changes in the wind-driven response related to stratification changes
 103 (Ralph and Niiler 1999; Rio et al. 2011). If a bin has a month with fewer than 10 drifter
 104 observations, the coefficients are not calculated but instead are filled via linear interpolation
 105 with neighboring bins for that month.

106 Next, having calculated a model for the wind-driven component of drogued drifters, we
 107 calculate the difference between the downwind ageostrophic, low-passed velocity of each
 108 drifter and $a\sqrt{\tau}$ interpolated to that drifter. By writing this difference as αW (Rio 2012),
 109 where W is the wind speed, we expect that $\alpha \sim 0$ for drogued drifters and $\alpha \sim 0.01$ for
 110 undrogued drifters (Pazan and Niiler 2001; Poulain et al. 2009).

111 In practice, we found that α tended to be larger; an examination of a subset of the data,
 112 3160 tether-strain drifters with known drogue loss, revealed that $\alpha=0.015\text{--}0.020$ after drogue
 113 loss. Drogue loss for the entire data set was determined automatically as follows: for each
 114 drifter with more than 10 days of data, the time series of α for $W > 1.5$ m/s was fit with a step
 115 function of the form $H=0, t < T_o; H=0.015, t \geq T_o$, with time T_o ranging from deployment
 116 to the final data point. The value of T_o that yielded the minimum value of $(\alpha - H)^2$ is the
 117 automatically-determined drogue loss time (Fig. 2a). The choice $\alpha=0.015$ after drogue loss
 118 lies near the lower range of observed values for the 3160 tether-strain drifters; larger values
 119 after drogue loss do not affect the drogue-off date determined by this approach.

120 The least-squares fit of a step function is our largest departure from Rio (2012), who
 121 chose the first time $\langle \alpha \rangle$ exceeded 0.003 as the drogue-off date, where $\langle \cdot \rangle$ is a running 100 day
 122 average. This change was motivated by Rio's methodology tending to estimate drogue loss

123 too early, due to cases in which $\langle \alpha \rangle$ temporarily exceeded 0.003 while the drogue was still
124 attached. This approach also allows us to automatically detect drogue presence for time
125 series less than 200 days long, which cannot be done with the Rio (2012) methodology;
126 there are 5416 drifters in the study period which collected observations for less than 200
127 days, contributing a potential additional 1326 drifter-years of velocity observations. Other
128 changes were less significant: Rio (2012) chose a model of the form $u' \sim \tau$ and used ERA
129 reanalysis rather than CCMP winds. The procedure described here was developed to closely
130 reproduce the drogue-off dates of the 3160 tether-strain drifters with known drogue loss.

131 Fig. 2 shows an example of a drifter currently identified as drogue-on for its lifetime
132 in the GDP metadata. The automatic reanalysis methodology (Fig. 2a) identifies drogue
133 loss 110 days after deployment. The time integral $\int \alpha dt$ (Fig. 2b) remains close to zero until
134 drogue loss, then increases quasi-linearly with time after that. After drogue loss, the drifter's
135 submergence (Fig. 2c) becomes noisy, but continues to register large values which – at the
136 recommendation of the manufacturer – were interpreted to indicate that the drogue was still
137 present and frequently submerging the surface float.

138 *b. Manual drogue detection reanalysis*

139 In retrospect, and combined with information from $\int \alpha dt$ (Fig. 2b), the submergence
140 record can be reevaluated to provide a more accurate drogue-off date. Additional information
141 can be derived from the radio frequency of drifter-satellite communications, which averages
142 401.65 MHz and in many cases displays a regular decrease of a few MHz during daylight due
143 to solar heating of the surface float and related thermal expansion of the crystal resonator,
144 which defines the frequency [Gary Williams, pers. comm.]. When the drogue is lost, the
145 magnitude of this diurnal variation often increases (Fig. 2d) due to less insulation from
146 submergences.

147 A second example of drogue loss is shown in Fig. 3. As with the first example the GDP
148 metadata states that the drogue was attached for the entire lifetime of this drifter. In this case

149 the automatic detection algorithm indicates drogue loss 94 days after deployment. However,
150 the increase in α was more gradual than in the first example, making exact determination
151 of drogue loss date difficult using the automatic methodology. Changes in the behavior of
152 submergence (Fig. 3c) and frequency (Fig. 3d) allow a more precise determination of drogue
153 loss, which occurred 39 days after deployment.

154 The GDP is now engaged in a manual reevaluation of drogue presence using all three of
155 these time series ($\int \alpha$, submergence or tether strain, and frequency) rather than solely using
156 submergence or tether strain as in the past, for all drifters in the altimeter time period.
157 These results are being included in periodic updates of the GDP metadata. The manual
158 reevaluation is being conducted in order of decreasing $T_b - T_a$, where T_b is the drogue-off
159 date according to the GDP metadata and T_a is the drogue-off date given by the automatic
160 reevaluation. As of 31 August 2012, a total of 10112 drifters (74%) have been manually
161 reevaluated.

162 3. Results and Discussion

163 According to GDP metadata prior to the automatic reanalysis conducted here (here-
164 after “**before**”), for the period 14 October 1992–30 November 2010, 62% of the velocity
165 measurements were collected by drogued drifters. After applying the automatic reanaly-
166 sis methodology (“**after**”), this fraction drops to 48%. Consistent with the time series of
167 velocity anomalies (Fig. 1) and with GLC11 (their Fig. 3), this error reached its peak in
168 mid-2006 (Fig. 4) when the fraction of drogued drifters must be reduced from 65% (**before**)
169 to 29% (**after**). This discrepancy diminishes to 37% (**before**) vs. 23% (**after**) by the end
170 of the study period (Fig. 4) as tether strain drifters were phased in and most of the older
171 submergence drifters had died. During this period, the number of drifters deployed per year
172 increased approximately linearly from ~ 500 in 1993–1994 to ~ 1000 in 2008–2010, with the
173 phase-in of the mini design starting in 2003.

174 The time-mean difference between undrogued and drogued drifters’ zonal component of
 175 velocity (ΔU) is generally aligned with the time mean zonal wind W_x (Fig. 5b). Consistent
 176 with previous studies (Pazan and Niiler 2001; Poulain et al. 2009), the magnitude of ΔU
 177 (**before**) is about 1% of W_x . However, this result is contaminated by the presence of misdi-
 178 agnosed undrogued drifters which increase the wind slip of the supposedly drogued drifters,
 179 thus decreasing $\Delta U/W_x$. This effect is most prominent in the region of strong winds south
 180 of 40°S (Fig. 5c). The automatic drogue reanalysis increases the globally averaged wind slip
 181 $\Delta U/W_x$ (**after**) to 1.5%. The increase over previous estimates of $\Delta U/W_x=1\%$ is due to the
 182 removal of a portion of the remaining undrogued drifters and to the larger relative fraction
 183 of Southern Ocean data collected since the early 2000s. This result suggests that wind slip of
 184 undrogued drifters is approximately 50% higher than was thought before. The discrepancy
 185 with Pazan and Niiler (2001) may also be due to a larger wind slip for undrogued mini
 186 drifters, as the mini design was phased in after that study; the global average slip of the
 187 older drifters after drogue loss is 1.4%, while the average slip of the mini drifters after drogue
 188 loss is 1.7%. By design, the two drifters move similarly while the drogue is attached.

189 The difference between time-mean zonal currents from “drogue on” drifter **before** and
 190 **after** is spatially linked to regions of strong winds (Fig. 5a), where the wind slip correction
 191 is stronger. In particular, the westward velocity component on the equatorward flanks of the
 192 subtropical gyres (North and South Equatorial Currents) is a few cm/s weaker **after** than
 193 **before**. Our new estimate of the eastward flow in the Antarctic Circumpolar Current
 194 (ACC) region 40–60°S is 4 cm/s weaker for the zonal mean (Fig. 5a), but the correction
 195 exceeds 10 cm/s at some locations, a result consistent with Rio (2012). The time variations
 196 in **before** currents in the ACC region (Fig. 1) contain significant spurious acceleration
 197 in the early 2000s [GLC11]. This acceleration was concurrent with the phase-in of the
 198 lighter and smaller mini drifter design [GLC11] that replaced the original, larger and more
 199 expensive design (Lumpkin and Pazos 2007). However, the acceleration is also present in
 200 the ACC speed evaluated separately from the larger original-design drifters and the newer

201 mini drifters (Fig. 1a), indicating that the switch in design was not the cause of these low
202 frequency variations. By using the results of the automatic reanalysis to remove previously
203 unidentified drogue loss, much of the low-frequency ACC variations disappear (Fig. 1b).

204 Although the exact cause of the drogue detection problem in the early 2000s is not clear,
205 it was likely associated with undocumented manufacturing changes that negatively affected
206 performance of the submergence sensor. The detection problem was greatly alleviated by the
207 phase-in of tether strain in the late 2000s, but not completely eradicated due to long-lived
208 drifters with faulty submergence (and, much more rarely, failure of a tether strain sensor).

209 The lifetime of the drogues can be quantified by their half-life, i.e., the number of days
210 after which half the drifters have lost their drogues. Because a drifter can die with the
211 drogue attached, providing a minimum estimate of the drogue lifetime, we calculate the
212 half-life iteratively: we first use the age at death for drifters which died with the drogue
213 still attached, and the lifetimes of the drogues for drifters which lost them. We then discard
214 age at death values which are less than the half-life and recalculate the half-life. While
215 there was a tendency for the resulting drogue half-life to decrease over the entire period
216 of the study, a sharp decrease was clearly associated with the switch from the older, more
217 robust and expensive drifter design to the less expensive mini drifter design (Fig. 6). The
218 older design had an overall mean drogue half-life of 325 days, while the mini drifters have
219 a mean drogue half-life of 104 days. The GDP is currently evaluating new tether materials
220 and tether/drogue attachment methods with the goal of increasing drogue lifetime without
221 significantly increasing cost. It should be emphasized that the drogue retention problem is
222 separate from the drogue detection problem: the original design drifters also suffered faulty
223 or noisy submergence sensors that degraded the quality of drogue detection (Fig. 1a).

224 For the 10112 drifters manually reevaluated so far, 7 have been declared “drogue status
225 uncertain from beginning” due to a combination of failed or ambiguous submergence/strain,
226 and ambiguous results from α and frequency. For the rest, drogue-loss dates from the
227 automatic method (T_a) and the manual reevaluation (T_m) compare favorably, with a median

228 $T_a - T_m$ of 1.25 days, mean of 32.5 days, and standard deviation of 112.7 days. The mean and
229 standard deviation are dominated by positive outliers. 637 drifters (6%) have $T_a - T_m > 90$,
230 i.e., manual drogue-loss date 90 days or earlier than given by the automatic reanalysis. There
231 are various reasons why the automatic routine was not accurate for these drifters. In some
232 cases α increased gradually (as in Fig. 3). In other cases α increased in two clearly-defined
233 steps, suggesting initial partial drogue loss (chosen in the manual reevaluation) followed later
234 by complete drogue loss at the date determined by the automatic methodology. Finally,
235 many drifters with large $T_a - T_m$ were located near the centers of the subtropical gyres,
236 where locally weak wind may result in insignificant slip while submergence and/or frequency
237 variations indicate drogue loss.

238 The results of the manual reevaluation are being included in updates of the GDP meta-
239 data. Drogue-off dates from this study's automatic drogue reanalysis, and ongoing re-
240 sults from the manual reevaluation, are available at [ftp://ftp.aoml.noaa.gov/phod/pub/
241 lumpkin/droguedetect/](ftp://ftp.aoml.noaa.gov/phod/pub/lumpkin/droguedetect/). Drifter-derived monthly climatological currents, available at [http:
242 //www.aoml.noaa.gov/phod/dac/dac_meanvel.php](http://www.aoml.noaa.gov/phod/dac/dac_meanvel.php) are updated to reflect this drogue re-
243 analysis.

244 *Acknowledgments.*

245 This research was supported by the NOAA's Climate Program Office, Climate Change
246 Data and Detection Program. RL was additionally supported by NOAA's Atlantic Oceanographic and Meteorological Laboratory.
247

REFERENCES

- 250 Atlas, R., R. N. Hoffman, J. Ardizzone, S. M. Leidner, J. C. Jusem, D. K. Smith,
251 and D. Gombos, 2011: A cross-calibrated, multiplatform ocean surface wind velocity
252 product for meteorological and oceanographic applications. **92**, 157–174, doi:10.1175/
253 2010BAMS2946.1.
- 254 Centurioni, L. R., P. P. Niiler, and D. K. Lee, 2009: Near-surface circulation in the South
255 China Sea during the winter monsoon. *Geophys. Res. Letters*, **36**, L06 605, doi:10.1029/
256 2008GL037076.
- 257 Fairall, C. W., E. F. Bradley, J. E. Hare, A. A. Grachev, and J. B. Edson, 2003: Bulk
258 parameterization of air-sea fluxes: Updates and verification for the COARE algorithm. *J.*
259 *Climate*, **16**, 571–591.
- 260 Grodsky, S. A., R. Lumpkin, and J. A. Carton, 2011: Spurious trends in global surface
261 drifter currents. *Geophys. Res. Letters*, **38**, L10 606, doi:10.1029/2011GL047393.
- 262 Hansen, D. and P.-M. Poulain, 1996: Quality control and interpolations of WOCE-TOGA
263 drifter data. *J. Atmos. Oceanic Technol.*, **13**, 900–909.
- 264 Lagerloef, G. S. E., G. T. Mitchum, R. B. Lukas, and P. P. Niiler, 1999: Tropical Pacific
265 near-surface currents estimated from altimeter, wind and drifter data. *J. Geophys. Res.*,
266 **104 (C10)**, 23 313–23 326.
- 267 Le Traon, P., F. Nadal, and N. Ducet, 1998: An improved mapping method of multisatellite
268 altimeter data. *J. Atmos. Oceanic Technol.*, **15**, 522–534.
- 269 Lumpkin, R. and M. Pazos, 2007: Measuring surface currents with Surface Velocity Program
270 drifters: the instrument, its data and some recent results. *Lagrangian Analysis and Predic-*

271 *tion of Coastal and Ocean Dynamics*, A. Griffa, A. D. Kirwan, A. Mariano, T. Özgökmen,
272 and T. Rossby, Eds., Cambridge University Press, chap. 2, 39–67.

273 Niiler, P. P., 2001: The world ocean surface circulation. *Ocean Circulation and Climate*,
274 G. Siedler, J. Church, and J. Gould, Eds., Academic Press, International Geophysics
275 Series, Vol. 77, 193–204.

276 Niiler, P. P., A. Sybrandy, K. Bi, P. Poulain, and D. Bitterman, 1995: Measurements of
277 the water-following capability of holey-sock and TRISTAR drifters. *Deep Sea Res.*, **42**,
278 1951–1964.

279 Pazan, S. E. and P. P. Niiler, 2001: Recovery of near-surface velocity from undrogued drifters.
280 *J. Atmos. Oceanic Technol.*, **18**, 476–489.

281 Piecuch, C. G. and T. A. Rynearson, 2012: Quantifying dispersion and connectivity of surface
282 waters using observational Lagrangian measurements. *J. Atmos. Oceanic Technol.*, **29** (8),
283 1127–1138, doi:10.1175/JTECH-D-11-00172.1.

284 Poulain, P.-M., R. Gerin, E. Mauri, and R. Pennel, 2009: Wind effects on drogued and
285 undrogued drifters in the eastern Mediterranean. *J. Atmos. Oceanic Technol.*, **26**, 1144–
286 1156, doi:10.1175/2008JTECHO618.1.

287 Ralph, E. A. and P. P. Niiler, 1999: Wind-driven currents in the Tropical Pacific. *J.*
288 *Phys. Oceanogr.*, **29**, 2121–2129.

289 Rio, M.-H., 2012: Use of altimetric and wind data to detect the anomalous loss of SVP-type
290 drifter’s drogue. *J. Atmos. Oceanic Technol.*, doi:10.1175/JTECH-D-12-00008.1.

291 Rio, M. H., S. Guinehut, and G. Larnicol, 2011: New CNES-CLS09 global mean dynamic
292 topography computed from the combination of GRACE data, altimetry and in situ mea-
293 surements. *J. Geophys. Res.*, **116**, C07 018, doi:10.1029/2010JCOO6505.

294 List of Figures

- 295 1 (a) Annually-low-passed time series of the geostrophic-removed zonal compo-
296 nent of drifter velocity in the circumpolar latitude band 40–60°S for the origi-
297 nal design drifters (solid, with light shaded error bar) and for the redesigned
298 mini drifters (dashed) (Lumpkin and Pazos 2007), both **before** the automatic
299 drogue reanalysis. (b) Annually-low-passed time series of the geostrophic-
300 removed zonal component of drifter velocity in the circumpolar latitude band
301 40–60°S **before** the automatic drogue reanalysis (dashed, dark standard error
302 bars) and **after** (solid, medium error bars), using all (original and mini) drifters. 16
- 303 2 (a) Time series of α (residual downwind component of drifter velocity divided
304 by wind speed) for drifter ID=45975, unfiltered (gray) and lowpassed with
305 a 100 day running mean (heavy black line) and lowpass with period cut-off
306 of 10 days (thin black line). Vertical dashed line indicates drogue-off date
307 determined by a least-squares fit of a step function (horizontal dashed lines).
308 Black dot indicates the first date that the 100 day lowpass exceeds 0.3%,
309 the criterion used by Rio (2012). (b) Cumulative sum of α used for manual
310 evaluation of results. Vertical dashed line repeated from (a). Sloping gray
311 lines indicate $\alpha=0.018$, a typical value after drogue loss, for visual reference.
312 (c) Submergence record from drifter. (d) Transmission frequency anomalies
313 (highpassed at 2 days).

17

- 314 3 (a) Time series of α (residual downwind component of drifter velocity divided
315 by wind speed) for drifter ID=62587, unfiltered (gray) and lowpassed with
316 a 100 day running mean (heavy black line) and lowpass with period cut-off
317 of 10 days (thin black line). Vertical dashed line indicates drogue-off date
318 determined by a least-squares fit of a step function (horizontal dashed lines).
319 Black dot indicates the first date that the 100 day lowpass exceeds 0.3%,
320 the criterion used by Rio (2012). (b) Cumulative sum of α used for manual
321 evaluation of results. Vertical dashed line repeated from (a). Sloping gray
322 lines indicate $\alpha=0.018$, a typical value after drogue loss, for visual reference.
323 (c) Submergence record from drifter. (d) Transmission frequency anomalies
324 (highpassed at 2 days). 18
- 325 4 (a) Number of drifters with (solid) and without (dashed) drogues, **before** (thin)
326 and **after** (thick) automatic drogue reanalysis. (b) Fraction of drifters with
327 drogues **before** (thin) and **after** (thick) reanalysis. 19
- 328 5 (a) Difference between mean zonal component of velocity (positive eastward)
329 of drifters thought to have drogues **before** the automatic reanalysis, and
330 mean zonal currents **after** (cm/s), 14 October 1992–30 November 2010, with
331 zero contour of time-mean zonal wind superimposed. (b) Drogue-off minus
332 drogue-on (**after**) zonal component of drifter velocity (shading; cm/s). Time
333 mean zonal wind superimposed (2 m/s contours), westerly/easterly wind is
334 solid/dashed, zero contour bold. (c) Time-longitude average, weighted by
335 observation density, of mean zonal wind interpolated to the drifters (shad-
336 ing, m/s) and drogue-off minus drogue-on zonal component of drifter velocity
337 (cm/s) **before** (dashed) and **after** (solid) automatic drogue reanalysis. 20

338 6 Drogue half-life as a function of deployment date, calculated in a one-year
339 sliding window for the original design drifters (solid) and for the redesigned
340 mini drifters (dashed); values are not shown if there were fewer than 50 drifters
341 of that type deployed in the one-year window. Open circles indicate values
342 for which more than half the drifters died with the drogues still attached. 21

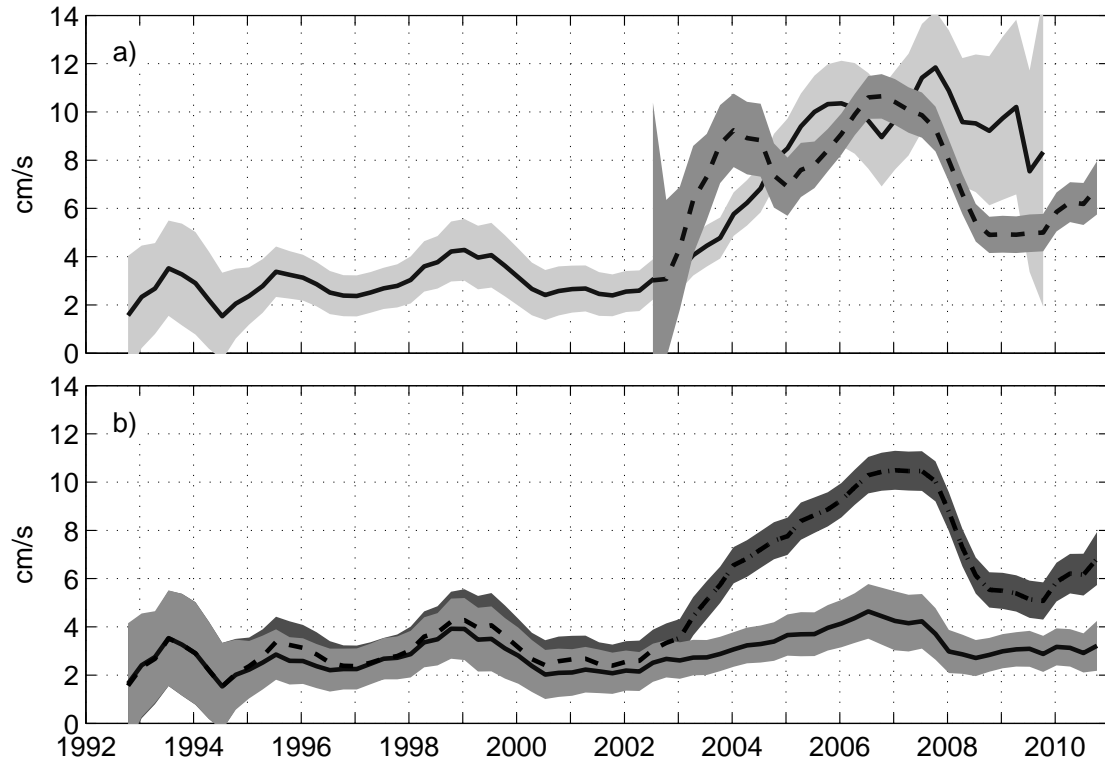


FIG. 1. (a) Annually-low-passed time series of the geostrophic-removed zonal component of drifter velocity in the circumpolar latitude band $40\text{--}60^\circ\text{S}$ for the original design drifters (solid, with light shaded error bar) and for the redesigned mini drifters (dashed) (Lumpkin and Pazos 2007), both **before** the automatic drogue reanalysis. (b) Annually-low-passed time series of the geostrophic-removed zonal component of drifter velocity in the circumpolar latitude band $40\text{--}60^\circ\text{S}$ **before** the automatic drogue reanalysis (dashed, dark standard error bars) and **after** (solid, medium error bars), using all (original and mini) drifters.

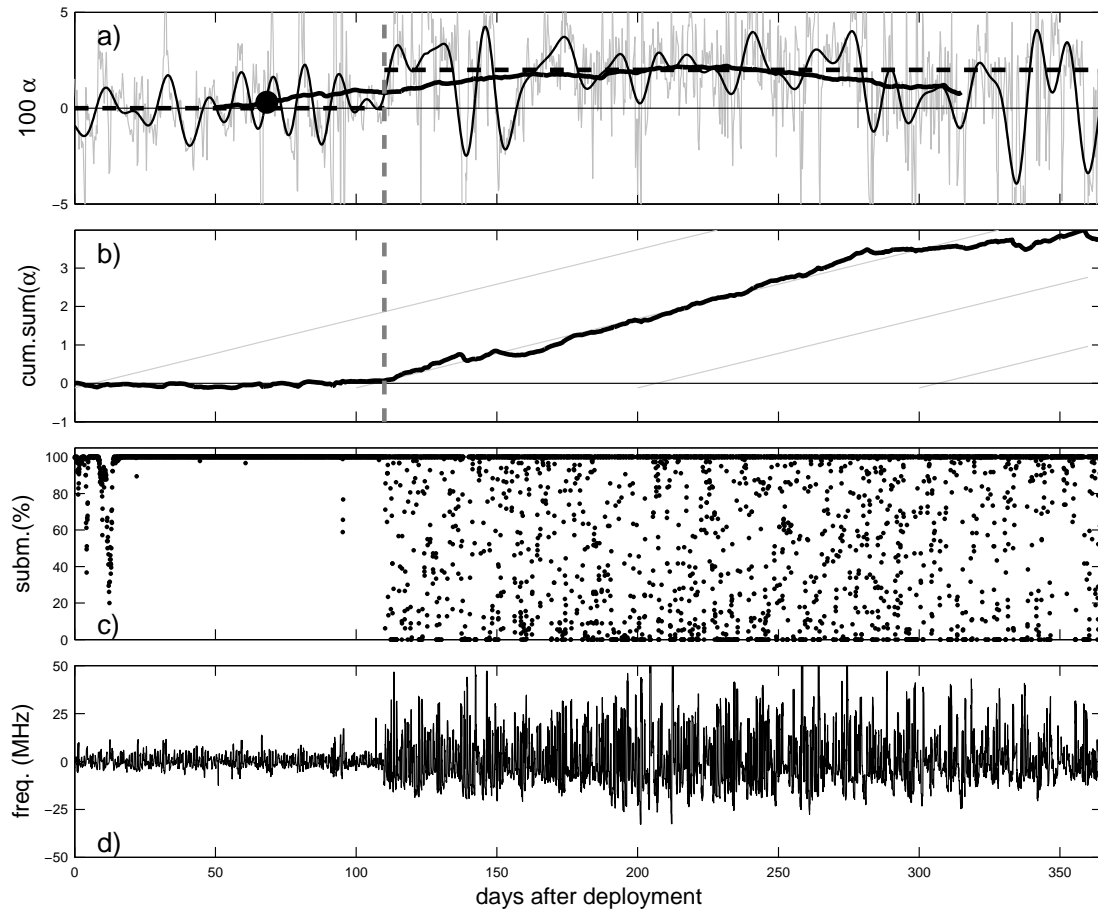


FIG. 2. (a) Time series of α (residual downwind component of drifter velocity divided by wind speed) for drifter ID=45975, unfiltered (gray) and lowpassed with a 100 day running mean (heavy black line) and lowpass with period cut-off of 10 days (thin black line). Vertical dashed line indicates drogue-off date determined by a least-squares fit of a step function (horizontal dashed lines). Black dot indicates the first date that the 100 day lowpass exceeds 0.3%, the criterion used by Rio (2012). (b) Cumulative sum of α used for manual evaluation of results. Vertical dashed line repeated from (a). Sloping gray lines indicate $\alpha=0.018$, a typical value after drogue loss, for visual reference. (c) Submergence record from drifter. (d) Transmission frequency anomalies (highpassed at 2 days).

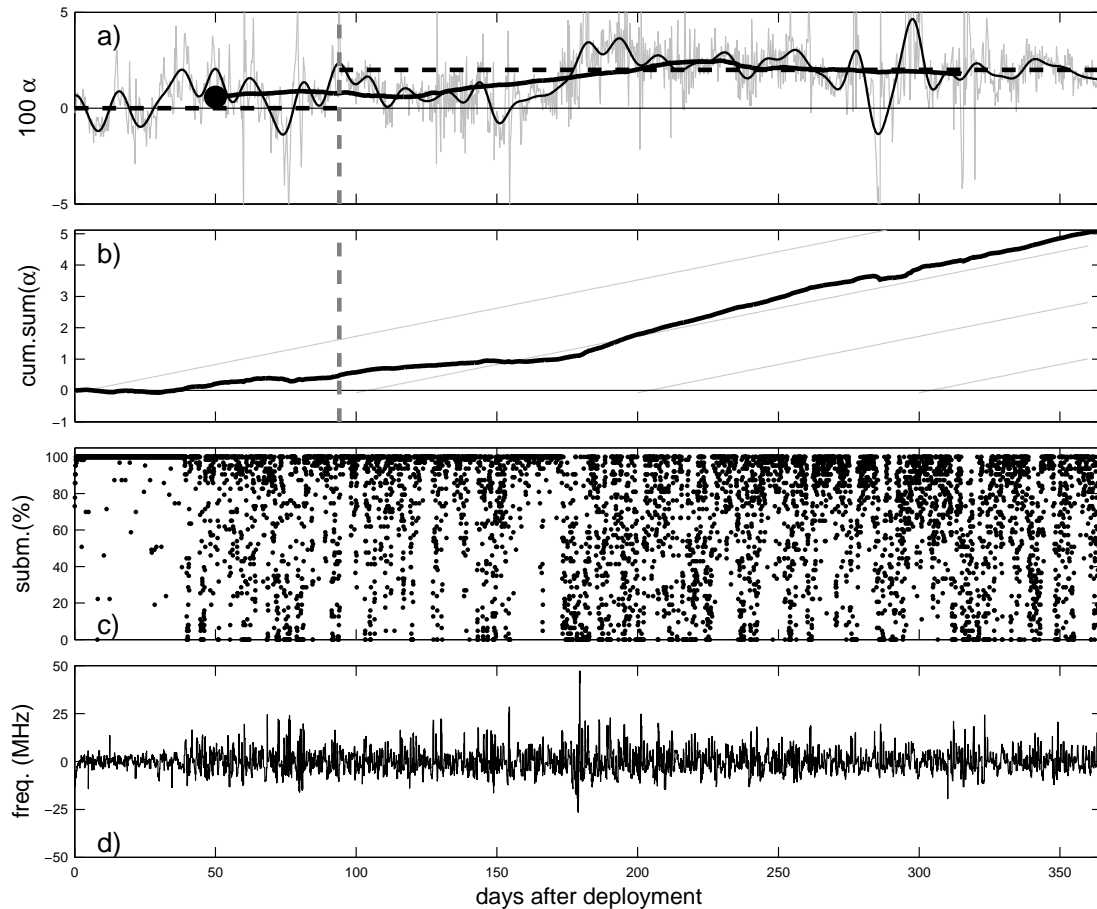


FIG. 3. (a) Time series of α (residual downwind component of drifter velocity divided by wind speed) for drifter ID=62587, unfiltered (gray) and lowpassed with a 100 day running mean (heavy black line) and lowpass with period cut-off of 10 days (thin black line). Vertical dashed line indicates drogue-off date determined by a least-squares fit of a step function (horizontal dashed lines). Black dot indicates the first date that the 100 day lowpass exceeds 0.3%, the criterion used by Rio (2012). (b) Cumulative sum of α used for manual evaluation of results. Vertical dashed line repeated from (a). Sloping gray lines indicate $\alpha=0.018$, a typical value after drogue loss, for visual reference. (c) Submergence record from drifter. (d) Transmission frequency anomalies (highpassed at 2 days).

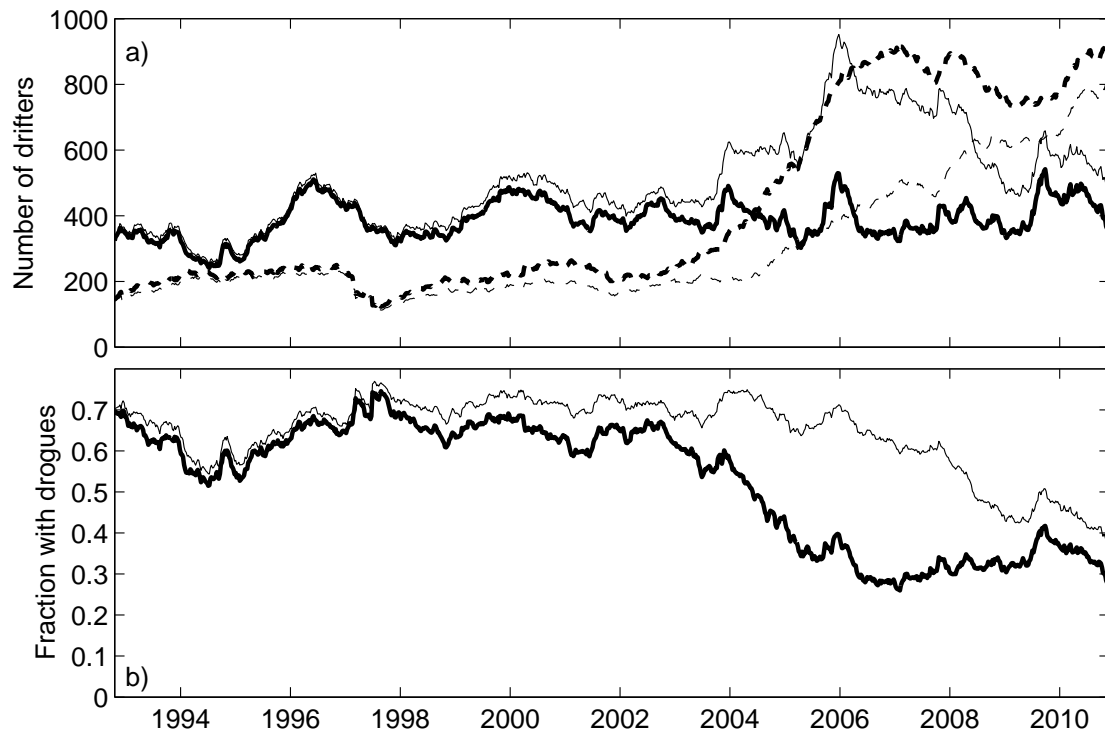


FIG. 4. (a) Number of drifters with (solid) and without (dashed) drogues, **before** (thin) and **after** (thick) automatic drogue reanalysis. (b) Fraction of drifters with drogues **before** (thin) and **after** (thick) reanalysis.

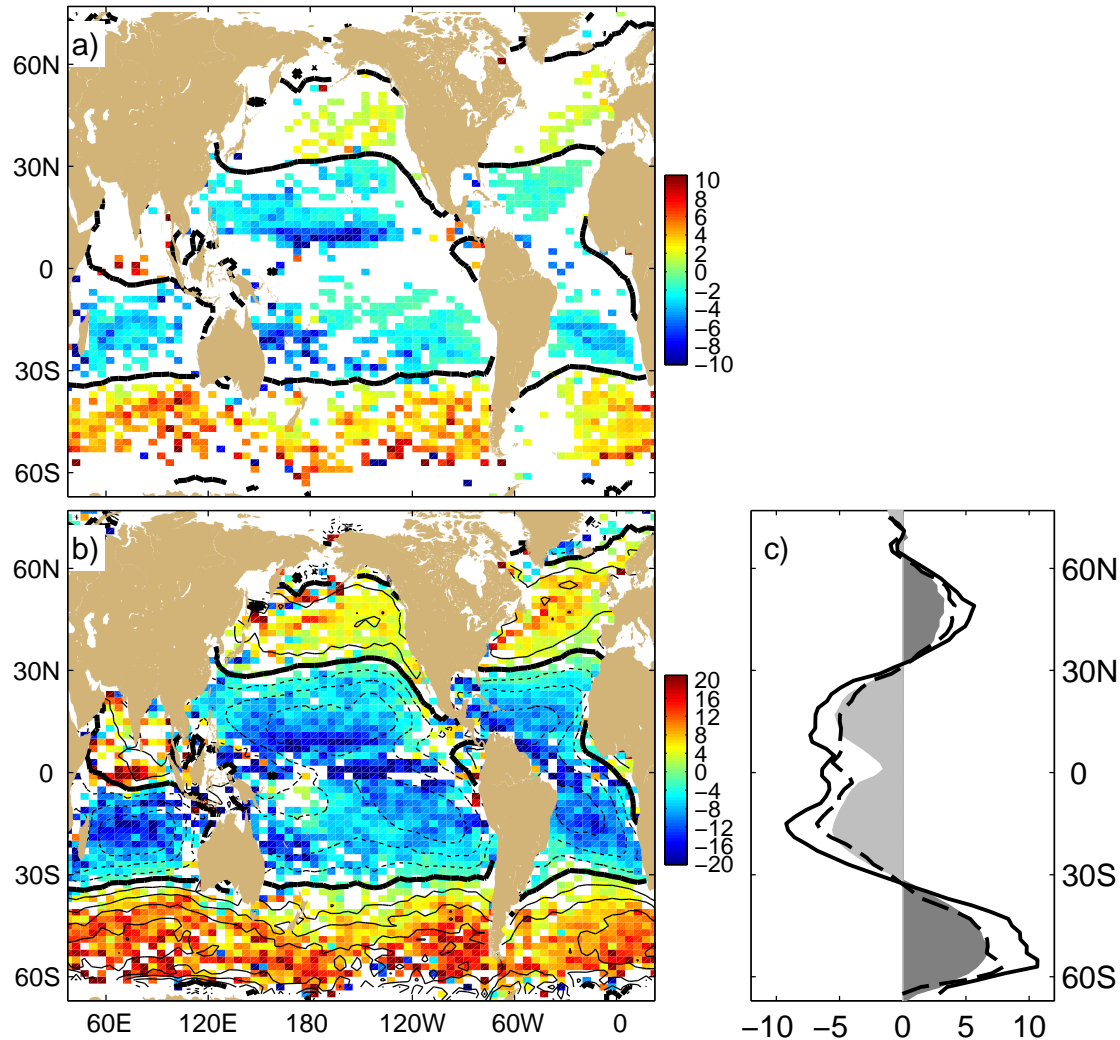


FIG. 5. (a) Difference between mean zonal component of velocity (positive eastward) of drifters thought to have drogues **before** the automatic reanalysis, and mean zonal currents **after** (cm/s), 14 October 1992–30 November 2010, with zero contour of time-mean zonal wind superimposed. (b) Drogue-off minus drogue-on (**after**) zonal component of drifter velocity (shading; cm/s). Time mean zonal wind superimposed (2 m/s contours), westerly/easterly wind is solid/dashed, zero contour bold. (c) Time-longitude average, weighted by observation density, of mean zonal wind interpolated to the drifters (shading, m/s) and drogue-off minus drogue-on zonal component of drifter velocity (cm/s) **before** (dashed) and **after** (solid) automatic drogue reanalysis.

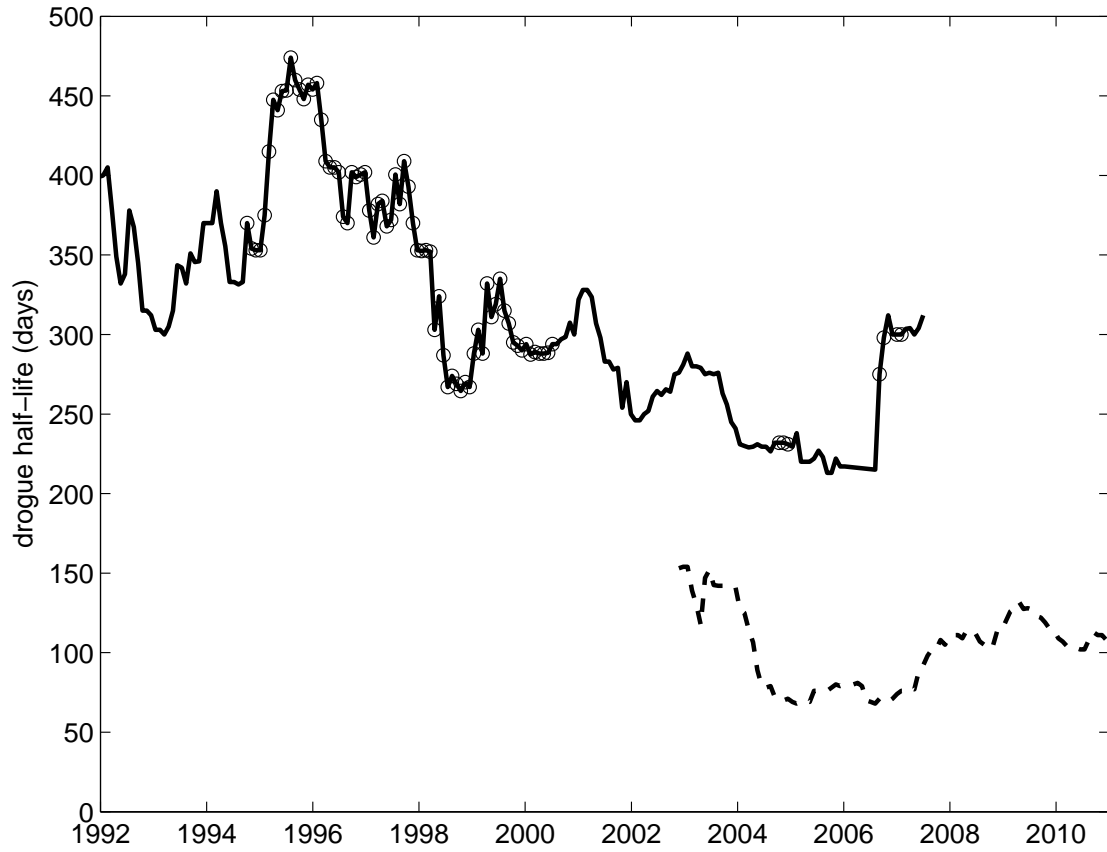


FIG. 6. Drogue half-life as a function of deployment date, calculated in a one-year sliding window for the original design drifters (solid) and for the redesigned mini drifters (dashed); values are not shown if there were fewer than 50 drifters of that type deployed in the one-year window. Open circles indicate values for which more than half the drifters died with the drogues still attached.